Mathematical Biosciences and Engineering

https://www.aimspress.com/journal/mbe

MBE, 22(11): 2897–2922.
DOI: 10.3934/mbe.2025107
Received: 10 April 2025
Revised: 04 September 2025
Accepted: 05 September 2025
Published: 17 September 2025

Research article

Fear induced coexistence in eco-epidemiological systems with infected prey

Rajesh Das[1] **and Sourav Kumar Sasmal**[1,2,*]

[1] Department of Applied Mathematics and Scientific Computing, IIT Roorkee, Uttarakhand 247667, India

[2] Mathematics, Faculty of Science, University of South Bohemia, Ceske Budejovice 37005, Czech Republic

* **Correspondence:** Email: sourav.sasmal@amsc.iitr.ac.in.

Abstract: The combined effects of ecological and disease characteristics are examined in eco-epidemiological models, which incorporate infectious illnesses into interaction models. We assumed in this article that the prey population is somewhat infected, and the predator benefits more from eating susceptible prey than from feeding on infected prey. Infected and susceptible prey are equally competitive for resources, and the predator consumes both at the same rate. We employed polar blow-up and time-scale desingularization techniques to tackle the singularity caused by frequency-dependent disease transmission at the origin in our model. For simplicity, we considered the linear functional response for interactions between prey and predators. We aimed to determine the influence of fear of predation on the eco-epidemiological system. According to our findings, there are two ways in which predation fear might support the coexistence of three populations: stable coexistence and oscillatory coexistence. Furthermore, our finding remained unchanged if we eliminated two presumptions: that susceptible and infected prey compete equally for resources and that predators consume both prey at identical rates. We also compared the outcomes by taking into account the growth with positive density dependency (Allee effect) and arrived at the same conclusion.

Keywords: eco-epidemiological system; coexistence; fear effect; polar blow-up; time-scale desingularization; Hopf bifurcation

1. Introduction

In ecology, Lotka [1] and Volterra [2] laid the groundwork for understanding the interactions between resource-consumer/prey-predator. This field has significantly enhanced with the addition of ecological complexity, which includes behavioral responses, spatial dynamics, and indirect effects. In the past few decades, researchers have concentrated on how non-consumptive effects influence

prey-predator dynamics [3–6]. Over the past century, many biological aspects have been incorporated into prey-predator interaction models. As an expansion of conventional ecological models, eco-epidemiological models incorporate disease dynamics into the investigation of species associations. The eco-epidemiological model was first introduced by Hadeler and Freedman [7]. After that, many works [8–10] have enriched this field. By decreasing prey populations or lowering predator fitness, diseases can drastically change predator-prey dynamics [11]. On the other hand, through modifications to host density, movement, and interaction variations, ecological interactions affect the rates at which diseases are transmitted [12, 13]. Eco-epidemiological models offer a thorough framework for comprehending the twin roles of disease and predation in forming ecosystems by merging ecological and epidemiological principles. These models are especially essential in the context of newly developing infectious diseases, which represent serious risks to ecosystem stability and biodiversity.

In "ecological and mathematical modeling", the fear effect, a non-consumptive impact of predators on prey has gained a lot of attention. In addition to direct predation, prey is frightened by predators, which changes their behavior, reproduction, foraging habits, and habitat utilization. These indirect impacts weigh equally with or even outweigh the direct consequences of predation [14–16], which can significantly impact population dynamics and ecological stability. Mathematical models that integrate the fear effect provide significant new insights into these complex interactions. Holling [17] established the foundation for integrating behavioral changes, including anxiety, into mathematical models with his early work [18] on functional response ideas. Indirectly predator impacts on prey populations, such as behavioral changes, were subsequently highlighted by Gilpin [19]. The investigation of fear dynamics in prey-predator interactions was made possible by these pioneering works. Krivan [20] created a two-patch prey-predator model that included habitat-switching (anti-predator) behavior of prey to illustrate the trade-offs between resource availability and safety. Wang et al. [21] introduced the fear effect in prey-predator dynamics by considering a reduction of the prey birth rate as a function of predator density. By incorporating the fear effect in the growth of prey populations subject to the Allee effect in an eco-epidemiological model, Sasmal [22] expanded and demonstrated how fear stabilizes or destabilizes system dynamics. Some recent works [23,24] incorporated fear in the eco-epidemiological system. These findings highlight how crucial it is to simulate fear effects in prey-predator systems because they offer vital information for managing resources, preserving biodiversity, and maintaining ecological stability.

How the disease spreads from the infected class to the susceptible class depends on social patterns and structures within the host population. Two categories of disease transmission rates exist in epidemiology, specifically the frequency-dependent transmission rate $[\phi(x) = \beta]$ and density-dependent transmission rate $[\phi(x) = \beta x]$ [11, 25], where β is the disease transmission rate and x is the host population density. In this study, we examine the frequency-dependent transmission of diseases. We employ a combination of time-scale desingularization and polar coordinate blow-up approaches to investigate the behavior of the system close to the extinction equilibrium at the origin, where the frequency-dependent transmission term leads to the singularity of the system. The blow-up transformation allows for a regular and thorough phase-space investigation around the origin by replacing a family of directions for the singular point. In this new framework, the transformed system is kept smooth and well-defined by a subsequent time parametrization, called time-scale desingularization. These mathematical methods have been successfully used in the study of

degenerate dynamics in planar systems and the desingularization of non-hyperbolic points [26, 27]. Additionally, they are relevant to ecological models that have boundary singularities or extinction, like ratio-dependent predator-prey systems [28], systems with Allee and hydra effects [29], and structured mosquito population models with singular behaviors [30]. Here, we use a comparable framework to verify the qualitative behavior of solutions close to the origin and conduct a thorough analysis of the extinction stage.

Another essential component of mathematical modeling that affects dynamics is functional response. Three categories of functional responses, namely, type I (linear), type II (hyperbolic), and type III (sigmoidal), were provided by Holling [18], which are widely used in the literature. For simplicity, we consider the Holling type I or the linear functional response in this study.

Hethcote et al. [31] assumed that infected prey is easier for predators to capture and demonstrated that, depending on the Allee effect in the predator, susceptible prey, infected prey, and predator can survive together under certain conditions. However, Sasmal and Chattopadhyay [34] studied a similar model with the belief that, even though the infected prey is easier for predators to acquire, it contributes less (or even negatively) to the growth of the predator than the consumption of susceptible prey. They demonstrated that, regardless of the Allee effects, coexistence between susceptible prey, infected prey, and predator is not possible, under such an assumption. The coexistence of susceptible prey, infected prey, and predator can be encouraged by intraspecific competition in predators [35], which is considered because of limited resources. Sasmal [22] concluded that fear can either produce an oscillating cohabitation between the susceptible prey, infected prey, and predator or stabilize the system at its interior equilibrium. In this article, our goal is to answer the following three questions:

1) Can fear of predators stabilize and promote the coexistence of susceptible prey and infected prey alongside predators in such a system?

2) What if we consider the Allee effect in the growth of the predator population?

3) What would happen if we relaxed the presumptions of equal resource competitiveness of preys and equal predator intakes of susceptible and diseased prey?

For this, we first consider the model studied by Sasmal et al. [35], without the Allee effect and where intraspecific competition induces additional death of predators, including fear of predators that reduces the birth rate of prey populations. We also discuss the results incorporating the Allee effect in the predator population, and remove the assumptions of equal resource competition of susceptible and infected prey and their equal consumption rates by the predator.

In Section 2, we develop our model based on the aforementioned assumptions. It also contains the boundedness and positivity of the suggested system, along with the table, which provides a quick overview of the model parameters and their default values for numerical simulation. The work is then aligned by considering two key ideas in Section 3, which are the disease-free demographic reproduction number of predators (R_d) and the basic reproduction number (R_0). Section 3 provides a detailed equilibrium analysis for the proposed system. We eliminate the origin's singularity and examine its stability using time-scale desingularization and polar blow-up techniques. In Section 4, we provide a detailed numerical simulation and validate our analytical findings. Also, we sum up all existence and stability regions of equilibria of our system and show the effect of the cost of fear of predators by bifurcation diagrams with respect to the fear coefficient. Lastly, we wrap up and discuss

our results with a few published research articles in Section 5. We also consider the positive density dependence growth of predators in our model and remove the assumptions of equal resource competition of susceptible prey and infected prey and their equal consumption rates by the predator. We conclude by providing the answers to the questions raised above in Section 6.

2. Model formulation

The prey population (N) is separated into two classes: susceptible prey (S) and infected prey (I), i.e., $N = S + I$. We assume that in the absence of infection, the prey population develops logistically with a birth rate r, natural death rate d_1, and carrying capacity $K = \dfrac{r - d_1}{d_2}$. Thus in the absence of infection and predation, the prey population follows the following equation:

$$\frac{dN}{dt} = (r - d_1)N\left(1 - \frac{N}{K}\right) \implies \frac{dS}{dt} = S(r - d_1 - d_2 S),$$

since $N = S + I = S$, as $I = 0$. d_2 is the death rate due to intraspecies competition in the susceptible prey population. Our model relies on the realistic assumption that only healthy, susceptible species can reproduce, as the physiological load of infection distracts an individual's energy from reproductive activities, whereas the competitive effect of infected individuals is captured indirectly by reducing resource availability for the reproducing members of the population. As the total population increases and moves only through the susceptible class, the mathematical formulation for this idea is given as:

$$\frac{dS}{dt} = S\Big(r - d_1 - d_2(S + I)\Big).$$

We consider frequency-dependent disease transmission with disease transmission rate β, and $\beta\dfrac{I}{N}S = \dfrac{\beta S I}{S + I}$ is the new infections per individual infected prey. It is assumed that the infection does not transmit vertically, and μI is the combined death of infected prey that includes natural death and death induced by the disease. Hence in the absence of predation, the above equation can be modified to the following system of equations for susceptible prey and infected prey:

$$\begin{aligned} \frac{dS}{dt} &= S\left(r - d_1 - d_2(S + I) - \frac{\beta I}{S + I}\right), \\ \frac{dI}{dt} &= I\left(\frac{\beta S}{S + I} - \mu\right). \end{aligned}$$

According to our model, susceptible prey are the only group that contributes to the population's reproductive output, whereas the infected prey are not able to reproduce because of physiological or behavioral abnormalities brought on by the disease. Nevertheless, the same limited natural resources, including food and space, are used by both susceptible individuals and individuals with illnesses. Therefore, by using resources that would otherwise be used for reproduction, infected prey have an indirect impact on the growth of susceptible prey species. The competition term, which is dependent on the overall prey density, is included in the growth equation of the susceptible prey, rather than directly contributing to the death of the diseased class, whose mortality is already dominated by the infection. A realistic ecological situation, where infected individuals create ecological pressure without aiding in population reproduction, is captured by this formulation [32–36].

Now, we assume that the birth rate (r) of the prey is reduced because of the predation fear by incorporating the fear function $f(k, P) = \dfrac{1}{1 + kP}$, where k is the fear strength, P is the density of predator, and the function $f(k, P)$ satisfies the six properties of fear functions discussed by Sasmal [22]. For simplicity, we consider that the predator population consumes both susceptible prey and infected prey at the same rate a (predators do not distinguish between infected prey and susceptible prey), and both interactions follow the mass action law with a linear functional response. Moreover, we presume that predator gain is higher by consuming the susceptible prey, compared to consuming the infected prey, and sometimes predator loss is there (negative effect) due to the consumption of infected prey [34–36]. For instance, in California, over 50,000 pelican birds perished between 1994–1996 as a result of consuming fish contaminated with a vibrio class of bacteria in the Salton Sea [37]. Also, eating fish infected with roundworms like Contracaecum caused malnourishment, weakened immunity, and digestive problems, which led to the deaths of several grey pelican birds around 2022 in India [38]. Under the above assumptions, the dynamics of the eco-epidemiological system can be governed by the following system of nonlinear first-order ordinary differential equations:

$$\begin{aligned} \frac{dS}{dt} &= S\left(\frac{r}{1+kP} - d_1 - d_2(S+I) - \frac{\beta I}{S+I} - aP\right), \\ \frac{dI}{dt} &= I\left(\frac{\beta S}{S+I} - aP - \mu\right), \\ \frac{dP}{dt} &= P\Big(bS + \alpha I - d_3\Big). \end{aligned} \tag{1}$$

Here d_3 is the natural death rate of the predator population. $b = ca$ and $\alpha = c'a$, where c (> 0) and c' (can be negative) are the biomass conversion efficiencies from susceptible and infected prey to predator, respectively. We assume $-\infty < c' \leq c$, and consequently $\alpha \in (-\infty, b]$ where $b > 0$. α and b are net gains of the predator by consuming infected prey and susceptible prey, respectively. That is, the gain of predators is more for consuming susceptible prey than the infected prey. For biological interpretations of the parameters used in system (1), and their default values for numerical simulation, see Table 1.

Table 1. Description of model parameters and their default values (for numerical simulation) for model (1).

Parameter	Biological interpretation	Value
r	Birth rate of susceptible prey	0.60
d_1	Natural death rate of susceptible prey	0.05
d_2	Death rate of prey due to intra-species/inter-species competition	0.05
d_3	Natural death rate of predators	0.40
μ	Death rate (natural + infected induced) of infected prey	0.45
β	Infection rate	0.90
a	Attack rate of predators	0.80
k	Coefficient of fear effect acting on the growth of susceptible prey	1.00
b	Net gain of predator for consuming susceptible prey	0.45
α	Net gain of predator for consuming infected prey	0.25

Theorem 2.1 (Positivity and boundedness of solutions)**.** *Assume the following conditions:*

$$d_3 > 0,\ r > d_1,\ -\infty < \alpha \le b,\ \text{with } b > 0.$$

Then system (1) *is positively invariant and uniformly ultimately bounded in* $\mathbb{R}^3_+$ *with the following properties:*

$$\begin{aligned}
&\limsup_{t\to\infty}\left\{S(t)\right\} \le \frac{r-d_1}{d_2},\\
&\limsup_{t\to\infty}\left\{S(t)+I(t)\right\} \le \frac{(r-d_1)(r-d_1+\mu)}{\mu d_2},\\
&\limsup_{t\to\infty}\left\{S(t)+I(t)+P(t)\right\} \le \frac{(r-d_1)(r-d_1+\mu)(d_3+\mu)}{\mu d_2 d_3}.
\end{aligned}$$

Proof. The solutions to the system $\left.\frac{dS}{dt}\right|_{S=0} = 0,\ \left.\frac{dI}{dt}\right|_{I=0} = 0,\ \left.\frac{dP}{dt}\right|_{P=0} = 0$ show that $S = 0,\ I = 0,\ P = 0$ are invariant manifolds. The continuity of the system implies system (1) is positively invariant in $\mathbb{R}^3_+$.

Now, for any $(S, I, P) \in \mathbb{R}^3_+$, and $S > \frac{r-d_1}{d_2}$, using the positive invariant property of system (1), we can write

$$\left.\frac{dS}{dt}\right|_{\left[S>\ \frac{r-d_1}{d_2}\right]} \le S\left[(r-d_1) - d_2 S - d_2 I - \frac{\beta I}{S+I} - aP\right] < 0.$$

Also,

$$\left.\frac{dS}{dt}\right|_{\left[S=\ \frac{r-d_1}{d_2},\ I=0,\ P=0\right]} = 0,\ \text{and}\ \left.\frac{dS}{dt}\right|_{\left[S=\ \frac{r-d_1}{d_2},\ I+P>0\right]} < 0.$$

This together implies

$$\limsup_{t\to\infty} S(t) \le \frac{r-d_1}{d_2}. \tag{2}$$

Considering $N(t) = S(t) + I(t)$, from the first two equations of system (1), we can write

$$\frac{dN}{dt} \le (r-d_1+\mu)S - \mu N.$$

From the limit (2), we can say that for any $\varepsilon > 0,\ \exists\ T(> 0)$ such that for all $t > T$, we have $S(t) \le \frac{r-d_1}{d_2} + \varepsilon$. This gives

$$\frac{dN}{dt} \le (r-d_1+\mu)\left(\frac{r-d_1}{d_2} + \varepsilon\right) - \mu N.$$

Now using the theory of differential inequality, and making $\varepsilon \to 0$, we write

$$\limsup_{t\to\infty} N(t) \le \frac{(r-d_1+\mu)\left(\frac{r-d_1}{d_2}\right)}{\mu} = \frac{(r-d_1)(r-d_1+\mu)}{\mu d_2}. \tag{3}$$

Now considering $Z(t) = N(t) + P(t)$, from the equations of system (1), we can write

$$\frac{dZ}{dt} \leq (r - d_1 + \mu)S + d_3N - d_3Z.$$

Limit (3) implies that for $\varepsilon > 0$, $\exists\, T' > 0$, such that for all $t > T'$, $N(t) \leq \dfrac{(r-d_1)(r-d_1+\mu)}{\mu d_2} + \varepsilon$. Thus combining the results obtained from the limits (2) and (3), and taking $T_1 = \max\{T, T'\}$, we can say that for all $t > T_1$,

$$\frac{dZ}{dt} \leq (r - d_1 + \mu)\left[\frac{r-d_1}{d_2} + \varepsilon\right] + d_3\left[\frac{(r-d_1)(r-d_1+\mu)}{\mu d_2} + \varepsilon\right] - d_3Z.$$

Now, using the theory of differential inequality, and making $\varepsilon \to 0$, we can write

$$\limsup_{t\to\infty} Z(t) \leq \frac{(r-d_1)(r-d_1+\mu)(d_3+\mu)}{\mu d_3 d_3}.$$

Thus the theorem follows. ∎

3. Mathematical analysis

A key concept in epidemiological models is the basic reproduction number $R_0 = \dfrac{\beta}{\mu}$, which is the ratio of secondary infections per unit time (β) over an average infectious period (μ). If $R_0 < 1$, the infection cannot spread; but, if $R_0 > 1$, it can spread over the population. The infection gets harder to control as R_0 increases. The disease-free demographic reproduction number [22] of predators, $R_d = \dfrac{b}{d_3}$, is another threshold parameter that is taken into account. This metric determines the proportion of expected offspring of typical individual predators throughout the course of their lives. In our further analysis, we will employ $\dfrac{\beta}{\mu} = R_0$ and $\dfrac{b}{d_3} = R_d$. In this section, we will present an in-depth investigation of the system (1).

Theorem 3.1 (Existence of equilibria)**.** *System* (1) *has five different types of equilibria, namely,*

1) *The extinction equilibrium,* $E_0 = (0, 0, 0)$, *which always exists.*

2) *The susceptible prey only equilibrium,* $E_S = \left(\dfrac{r-d_1}{d_2}, 0, 0\right)$, *which exists if* $r > d_1$.

3) *The infected prey free equilibrium,* $E_{SP} = \left(\dfrac{1}{R_d}, 0, P_1\right)$, *which exists if* $R_d > \dfrac{d_2}{r-d_1}$ *where*

$$P_1 = \frac{-\left[aR_d + k\left(d_1R_d + d_2\right)\right] + \sqrt{\left[aR_d - k\left(d_1R_d + d_2\right)\right]^2 + 4akrR_d^2}}{2akR_d}.$$

4) *The predator free equilibrium,* $E_{SI} = \left(S_1, (R_0 - 1)S_1, 0\right)$, *which exists if* $1 < R_0 < 1 + \dfrac{r-d_1}{\mu}$, *where* $S_1 = \dfrac{(r-d_1) - \mu(R_0-1)}{d_2R_0}$.

5) The coexistence equilibria, $E^* = (S^*, I^*, P^*)$, *where*

$$S^* = \frac{1-\alpha X^*}{R_d},\ I^* = \frac{bX^*}{R_d},\ P^* = \frac{\mu}{a}\left[\frac{R_0(1-\alpha X^*)}{1+(b-\alpha)X^*} - 1\right], \tag{4}$$

and X^* *is the root of the quadratic equation*

$$Ax^2 + Bx + C = 0, \tag{5}$$

where

$$\begin{aligned} A &= d_2(b-\alpha)\left[b(a-\mu k) - a\alpha - \alpha k\mu(R_0-1)\right], \\ B &= -\mu^2\alpha k R_d (R_0-1)^2 - \mu\left[\{k(b\mu+\alpha d_1) - a(b-\alpha)\}R_d - kd_2(b-2\alpha)\right](R_0-1) \\ &\quad - \{a(b-\alpha)(r-d_1) + bd_1\mu k\}R_d + d_2\left[2a(b-\alpha) - b\mu k\right], \\ C &= \mu^2 k R_d (R_0-1)^2 + \mu\{kd_2 + R_d(a+d_1k)\}(R_0-1) - a\{(r-d_1)R_d - d_2\}. \end{aligned}$$

Now, if $0 < X^* < \dfrac{R_0-1}{b+\alpha(R_0-1)}$, *then the coexistence equilibrium* (E^*) *exists.*

Proof. System (1), can be written as

$$\frac{dS}{dt} = S \times F^{(1)}(S,I,P), \quad \frac{dI}{dt} = I \times F^{(2)}(S,I,P), \quad \frac{dP}{dt} = P \times F^{(3)}(S,I,P),$$

where

$$\begin{aligned} F^{(1)}(S,I,P) &= \frac{r}{1+kP} - d_1 - d_2(S+I) - \frac{\beta I}{S+I} - aP, \\ F^{(2)}(S,I,P) &= \frac{\beta S}{S+I} - aP - \mu, \text{ and} \\ F^{(3)}(S,I,P) &= bS + \alpha I - d_3. \end{aligned}$$

(i) Clearly, $E_0 = (0,0,0)$ always exists.

(ii) For E_S, we have $F^{(1)}(S,0,0) = 0 \implies S = \dfrac{r-d_1}{d_2}$, which exists if $r > d_1$.

(iii) For E_{SP}, we have $F^{(1)}(S,0,P) = 0$ and $F^{(3)}(S,0,P) = 0$, which give $S = \dfrac{1}{R_d}$, and P is the positive root of the quadratic equation

$$akR_dx^2 + [d_2k + R_d(a+d_1k)]\,x + [d_2 - (r-d_1)R_d] = 0.$$

The above equation has a unique positive root if $d_2 - (r-d_1)R_d < 0$, i.e., iff $R_d > \dfrac{d_2}{r-d_1}$.

(iv) For E_{SI} we have $F^{(1)}(S,I,0) = 0$ and $F^{(2)}(S,I,0) = 0$. This give $S = \dfrac{(r-d_1)-\mu(R_0-1)}{d_2R_0} = S_1$ (say), and $I = (R_0-1)S_1$. Thus the equilibrium E_{SI} exists iff $1 < R_0 < 1 + \dfrac{r-d_1}{\mu}$.

(v) Now, for the coexisting equilibrium E^*, we have the equation $F^{(i)}(S,I,P) = 0$, for $i = 1,2,3$. By some mathematical calculations, we have the expressions for S^*, I^*, and P^* given in Theorem 3.1, where X^* is the positive root of Eq (5), which can have zero, one, or two positive roots depending

on its coefficients. The explicit conditions for the signs of the coefficients A, B, C of Eq (5) are given in Appendix A.

Now, for positive roots X^* of Eq (5), the existence of E^* required $X^* < \frac{1}{\alpha}$ and $X^* < \frac{R_0 - 1}{b + \alpha(R_0 - 1)}$, (for the positivity of S^* and P^*).

If $\alpha > 0$, then clearly E^* exists if $X^* < \min\left\{\frac{1}{\alpha}, \frac{R_0 - 1}{b + \alpha(R_0 - 1)}\right\} = \frac{R_0 - 1}{b + \alpha(R_0 - 1)}$. Also, if $\alpha < 0$, then S^* and I^* are always positive, and consequently the interior equilibrium E^* exists for $X^* < \frac{R_0 - 1}{b + \alpha(R_0 - 1)}$. Thus, for $-\infty < \alpha \leq b$, the interior equilibrium E^* exists if $0 < X^* < \frac{R_0 - 1}{b + \alpha(R_0 - 1)}$.

∎

Theorem 3.2 (Stability of extinction equilibrium)**.** *The extinction equilibrium E_0 is globally asymptotically stable if $r \leq d_1$, and a saddle point if $r > d_1$.*

Proof. To study the stability of the extinction equilibrium E_0, we first consider the predator-free system:

$$\begin{aligned} \frac{dS}{dt} &= S\left(r - d_1 - d_2(S + I) - \frac{\beta I}{S + I}\right), \\ \frac{dI}{dt} &= I\left(\frac{\beta S}{S + I} - \mu\right). \end{aligned} \tag{6}$$

As $(S, I) = (0, 0)$ is a singular point of system (6), we cannot use linear stability analysis at the point. To tackle this, we use the time-scale desingularization $\frac{d\tau}{dt} = (S + I)^{-1}$. This changes system (6) to

$$\begin{aligned} \frac{dS}{d\tau} &= (r - d_1)S^2 + (r - d_1 + \beta)SI - d_2 S(S + I)^2, \\ \frac{dI}{d\tau} &= (\beta - \mu)SI - \mu I^2. \end{aligned} \tag{7}$$

Previously the singular point in system (6), $(S, I) = (0, 0)$, became an equilibrium point of system (7). For system (7), only the vector field is multiplied by $(S + I)$; nevertheless, for systems (6) and (7), the solutions are unchanged. Since there are no linear terms of S, I in the right-hand side of system (7), the eigenvalues of the Jacobian at $(0, 0)$ are both zero, and we must employ some blow-up approach to further analyze the stability at $(0, 0)$.

We use the polar blow-up technique for which we take the coordinate transformations $S = \rho cos\theta$ and $I = \rho sin\theta$, which yield $\rho^2 = S^2 + I^2$ and $\theta = tan^{-1}\left(\frac{I}{S}\right)$. Differentiating with respect to τ, and writing $\frac{d}{d\tau} = (\dot{})$, we obtain the relations $\dot{\rho} = cos\theta\dot{S} + sin\theta\dot{I}$ and $\dot{\theta} = \frac{1}{\rho}\left(cos\theta\dot{I} - sin\theta\dot{S}\right)$. System (7) becomes

$$\begin{aligned} \dot{\rho} &= \left[cos^2\theta\,(sin\theta + cos\theta)\,(r - d_1 - \beta + \mu) + (\beta - \mu)cos\theta - \mu sin\theta\right]\rho^2 - d_2 cos^2\theta\,(1 + sin2\theta)\,\rho^3, \\ \dot{\theta} &= -sin\theta cos\theta\,(sin\theta + cos\theta)\left[(r - d_1 - b + \mu)\,\rho - d_2\,(cos\theta + sin\theta)\,\rho^2\right]. \end{aligned}$$

Using the time-scale transformation $\frac{d\eta}{d\tau} = \rho$ (which multiplies the vector field of the above system by ρ), and writing $\frac{d}{d\eta} = (')$, we have

$$\begin{aligned} \rho' &= \left[cos^2\theta\,(sin\theta + cos\theta)\,(r - d_1 - \beta + \mu) + (\beta - \mu)cos\theta - \mu sin\theta\right]\rho - d_2 cos^2\theta\,(1 + sin2\theta)\,\rho^2, \\ \theta' &= -sin\theta cos\theta\,(sin\theta + cos\theta)\,[(r - d_1 - b + \mu) - d_2\,(cos\theta + sin\theta)\,\rho]\,. \end{aligned}$$

The singular directions of the above system are given by $\theta' = 0$. While $0 < \rho << 1$, we can write $\theta' = 0 \implies sin\theta cos\theta\,(sin\theta + cos\theta) = 0$. We are interested for $\theta \in \left[0, \frac{\pi}{2}\right]$ in the positivity of S and I. We obtain $\theta_1 = 0$ and $\theta_2 = \frac{\pi}{2}$.

Now, along $\theta = \theta_1$, $\rho' = (r - d_1)\rho - d_2\rho^2 \approx (r - d_1)\rho$, since $0 < \rho << 1$. Then we have $\rho' < 0$ if $r \le d_1$, and $\rho' > 0$ if $r > d_1$. Again, along $\theta = \theta_2$, $\rho' = -\mu\rho$, which is always negative.

This leads us to the conclusion that if $r \le d_1$, there will be attracting parabolic trajectories in the first quadrant $\mathbb{R}^2_+$, which will proceed to $(0, 0)$ (see Figure 1 (a),(c)). Also, if $r > d_1$, there are elliptic trajectories in the first quadrant, which will go outward from the origin along the S-axis, and be attracted to the origin along the I-axis. This suggests that $(0, 0)$ is a saddle point when $r > d_1$ and globally asymptotically stable if $r \le d_1$.

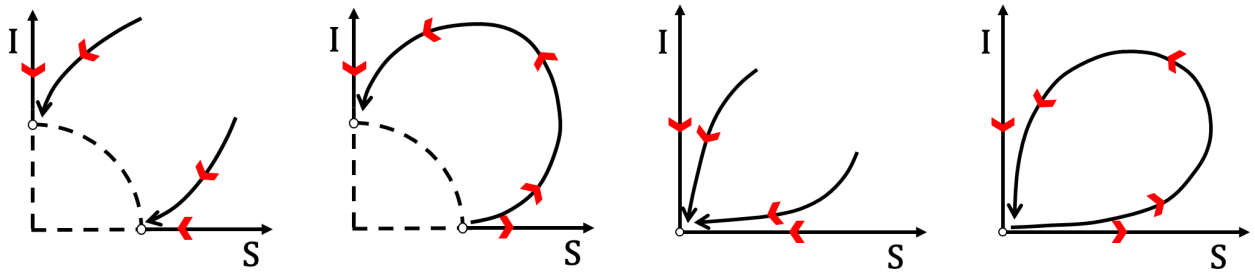

(a) Blow-up case for $r \le d_1$. (b) Blow-up case for $r > d_1$. (c) Blow-down case for $r \le d_1$. (d) Blow-down case for $r > d_1$.

Figure 1. The blow-up and blow-down scenarios for the origin of the SI system. The origin is stable if $r \le d_1$, and a saddle for $r > d_1$.

Now for the extinction equilibrium E_0 of system (1), consider $S = 0$, $I = 0$, and then the third equation becomes $\frac{dP}{dt} = -dP$. This shows that the predator will decay and go extinct in the absence of prey. Therefore, we conclude that if $r \le d_1$, E_0 is globally asymptotically stable in $\mathbb{R}^3_+$, and a saddle if $r > d_1$. ∎

Theorem 3.3 (Stability of boundary equilibria)**.** *The stability conditions for the boundary equilibria of system* (1) *are given as follows:*

i. The susceptible prey only equilibrium (E_S) *is locally asymptotically stable (LAS) if* $R_0 < 1$ *and* $R_d < \frac{d_2}{r - d_1}$.

ii. The infection free equilibrium (E_{SP}) is LAS if $R_0 < 1 + \dfrac{aP_1}{\mu}$.

iii. The predator free equilibrium (E_{SI}) is LAS if

$$R_0 > 1 \text{ and } R_d < \frac{bd_2R_0}{[b+\alpha(R_0-1)]\left[(r-d_1)-\mu(R_0-1)\right]}.$$

Proof. To prove the stability of boundary and interior equilibria, we use the following Jacobian:

$$J = \begin{pmatrix} F^{(1)} + S \times F_S^{(1)} & S \times F_I^{(1)} & S \times F_P^{(1)} \\ I \times F_S^{(2)} & F^{(2)} + I \times F_I^{(2)} & I \times F_P^{(2)} \\ P \times F_S^{(3)} & P \times F_I^{(3)} & F^{(3)} + P \times F_P^{(3)} \end{pmatrix}, \tag{8}$$

where $F_S^{(i)} = \dfrac{\partial}{\partial S}\left[F^{(i)}(S,I,P)\right]$, $F_I^{(i)} = \dfrac{\partial}{\partial I}\left[F^{(i)}(S,I,P)\right]$, and $F_P^{(i)} = \dfrac{\partial}{\partial P}\left[F^{(i)}(S,I,P)\right]$, for $i = 1, 2, 3$. The elements of the above Jacobian are given in Appendix B.

i. At the susceptible prey only equilibrium E_S, the eigenvalues of Jacobian (8) are $-(r-d_1)$ (<0), $\mu(R_0-1)$, and $b\left[\dfrac{(r-d_1)}{d_2} - \dfrac{1}{R_d}\right]$; Clearly, if $R_0 < 1$ and $R_d < \dfrac{d_2}{r-d_1}$, the equilibrium E_S is locally asymptotically stable.

ii. At the infection free equilibrium E_{SP}, one eigenvalue is $\mu(R_0-1) - aP_1$, and the other two eigenvalues are the roots of the quadratic equation

$$\lambda^2 + \frac{d_2}{R_d}\lambda + \frac{bP_1}{R_d}\left[a + \frac{rk}{(1+kP_1)^2}\right] = 0,$$

where $P_1 = \dfrac{-\left[aR_d + k\left(d_1R_d + d_2\right)\right] + \sqrt{\left[aR_d - k\left(d_1R_d + d_2\right)\right]^2 + 4akrR_d^2}}{2akR_d}$. Both the roots of the above equation are always negative (negative real parts). Thus the equilibrium E_{SP} is locally asymptotically stable if

$$\mu(R_0-1) - aP_1 < 0 \iff R_0 < 1 + \frac{aP_1}{\mu}.$$

iii. For the predator free equilibrium E_{SI}, we have $\alpha(R_0-1)S_1 + bS_1 - \dfrac{b}{R_d}$ as one eigenvalue of Jacobian (8), and the other two eigenvalues are the roots of the quadratic equation

$$\lambda^2 + d_2S_1\lambda + d_2\mu(R_0-1)S_1 = 0.$$

Both the roots of the above equation have negative real parts if $R_0 > 1$. Thus the equilibrium E_{SI} is locally asymptotically stable if

$$R_0 > 1 \text{ and } S_1 < \frac{b}{R_d\left[b+\alpha(R_0-1)\right]}$$

$$\text{i.e., iff } R_0 > 1 \text{ and } R_d < \frac{bd_2R_0}{[b+\alpha(R_0-1)]\left[(r-d_1)-\mu(R_0-1)\right]}.$$

∎

Theorem 3.4 (Stability of coexistence equilibrium)**.** *The coexisting equilibrium E^* is locally asymptotically stable if*

$$\frac{S^*\left[brk\mu R_0 I^* P^* - d_2 R_d (S^*+I^*)\left\{brkP^*(S^*+I^*)+\mu d_2 R_0 I^*(1+kP^*)^2\right\}\right]}{abd_2 R_d P^*(S^*+I^*)} < \left[(S^*+I^*)(1+kP^*)\right]^2 < \frac{brk\mu R_0}{ad_2 R_d(b-\alpha)}.$$

Proof. To prove the stability conditions of the coexistence equilibrium E^*, we have the characteristic equation of the Jacobian matrix (8):

$$\lambda^3 + A_1\lambda^2 + A_2\lambda + A_3 = 0,$$

where

$$\begin{aligned} A_1 &= d_2 S^* \quad (>0), \\ A_2 &= \frac{abP^*}{R_d} + \frac{brkS^*P^*}{(1+kP^*)^2} + \frac{\mu d_2 R_0 S^* I^*}{(S^*+I^*)} \quad (>0), \\ A_3 &= S^* I^* P^* \left[\frac{brk\mu R_0}{R_d\left[(S^*+I^*)(1+kP^*)\right]^2} - ad_2(b-\alpha)\right]. \end{aligned}$$

According to the Routh-Hurwitz criteria, E^* is locally asymptotically stable if $A_3 > 0$ and $A_1A_2 - A_3 > 0$.

$$A_3 > 0 \implies \left[(S^*+I^*)(1+kP^*)\right]^2 < \frac{brk\mu R_0}{ad_2 R_d(b-\alpha)}.$$

$$A_1A_2 - A_3 = S^*\left[d_2(S^*+I^*)\left\{abP^* + \frac{d_2\mu R_0 S^* I^*}{(S^*+I^*)^2}\right\} + \frac{bd_2 rkS^*P^*}{(1+kP^*)^2} - \frac{brk\mu R_0 I^* P^*}{R_d(S^*+I^*)^2(1+kP^*)^2}\right].$$

Thus,

$$A_1A_2 - A_3 > 0 \implies \frac{brk\mu R_0 I^* P^*}{R_d(S^*+I^*)^2(1+kP^*)^2} < d_2(S^*+I^*)\left\{abP^* + \frac{d_2\mu R_0 S^* I^*}{(S^*+I^*)^2}\right\} + \frac{bd_2 rkS^*P^*}{(1+kP^*)^2},$$

which gives

$$\left[(S^*+I^*)(1+kP^*)\right]^2 > \frac{S^*\left[brk\mu R_0 I^* P^* - d_2 R_d\,(S^*+I^*)\left\{brkP^*(S^*+I^*)+\mu d_2 R_0 I^*(1+kP^*)^2\right\}\right]}{abd_2 R_d P^*(S^*+I^*)}.$$

∎

4. Numerical simulation

In this section, we provide some numerical simulations to validate our analytical results. We plotted a variety of graphs using MATLAB software.

The existence and stability of various equilibria of system (1) are shown in Figure 2 on the R_0 versus R_d parametric plane. We divided the entire plane into nine regions according to our analytical findings. In Figure 2, the magenta-colored horizontal line represents $R_d = \dfrac{d_2}{r-d_1}$, the left cyan-colored vertical

line represents $R_0 = 1$, and the right cyan-colored vertical line represents $R_0 = 1 + \dfrac{r - d_1}{\mu}$. The blue-colored curve represents $R_0 = 1 + \dfrac{aP_1}{\mu}$, where P_1 is given in Theorem 3.1, and the red-colored curve represents $R_d = \dfrac{bd_2R_0}{[b + \alpha(R_0 - 1)]\,[r - d_1 - \mu(R_0 - 1)]}$. As the axial equilibrium (E_S) exists for $r > d_1$, it exists in all nine regions but is stable only in region 1 since we are taking default parameter values from Table 1, where $r > d_1$. The predator free equilibrium E_{SI} exists in regions 2, 4, and 6–8 but is stable only in regions 2 and 4. Similarly, the infection free equilibrium E_{SP} exists in regions 4–9, however, it is only stable in regions 8 and 9. Region 6 represents the oscillatory coexistence of susceptible prey, infected prey, and predator. In contrast, region 7 represents the stable coexistence between susceptible prey, infected prey, and predator. In region 3, E_S exists but is unstable and in region 5, E_{SP} exists but is unstable.

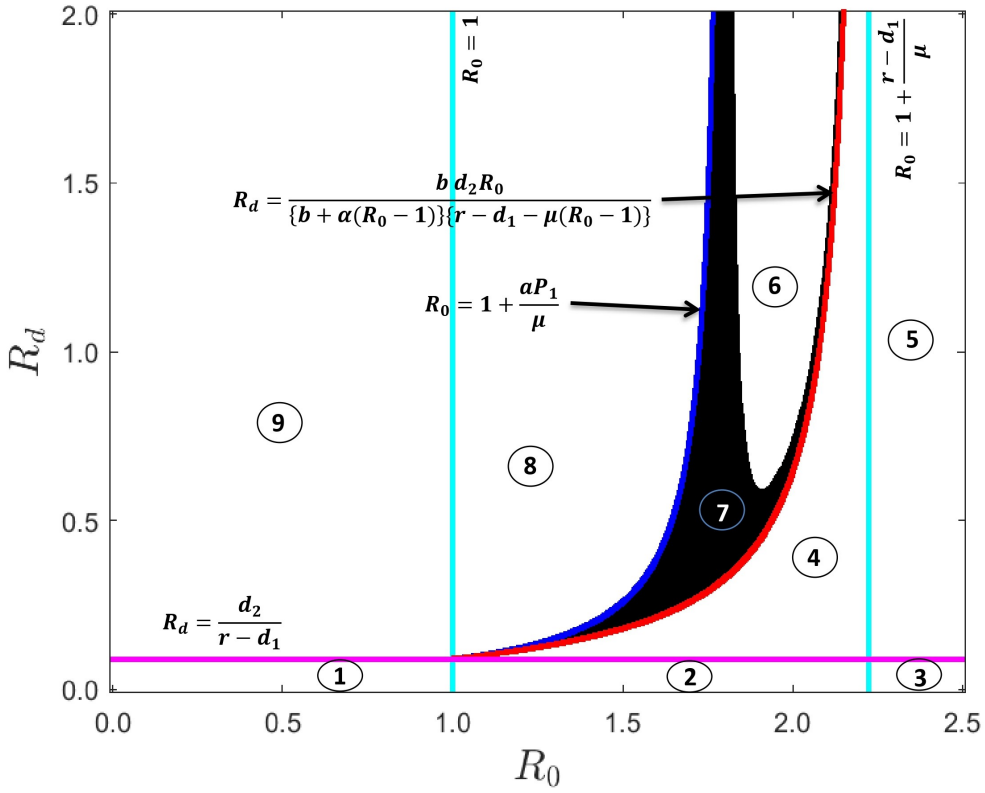

Figure 2. The existence and stability regions of different equilibria of system (1) in the R_0 vs. R_d plane, where all other parameters are taken from Table 1. In the figure, region 1 represents the existence and stability of E_S, whereas in regions 2 and 4, E_{SI} exists and is stable. In regions 8 and 9, E_{SP} exists and is stable. The black region 7 represents the existence and stability of E^*, whereas region 6 represents oscillatory coexistence. Region 3 represents the unstable existence of E_S, and region 5 represents the unstable existence of E_{SP}.

Figure 3 shows the bifurcation diagram of populations of system (1) with respect to the cost of fear of predators (k) as the bifurcating parameter. Initially, when the strength of fear is small, E_{SP} is stable.

As we increase the strength of fear, stable interior E^* appears. However, if we increase it further, the interior will lose its stability via Hopf bifurcation and oscillatory coexistence. System (1) experiences a supercritical Hopf bifurcation with respect to the bifurcating parameter k.

The Hopf bifurcation in a three-dimensional system is difficult to investigate mathematically due to the complicated nature of the system's solution expressions and other considerations. Although it is challenging to determine the critical value of k at which the Hopf bifurcation occurs, we can numerically validate the bifurcation conditions and their transversality requirement for the parameters used in the numerical simulation, as specified in the paper. When the Routh-Hurwitz determinant disappears and the Jacobian at the interior has two purely imaginary eigenvalues and one eigenvalue with a negative real portion, the Hopf bifurcation will take place in a three-dimensional system. To guarantee that the pair of imaginary eigenvalues crosses the imaginary axis with nonzero speed and does not stay on the imaginary axis, the transversality condition is crucial for the Hopf bifurcation. Appendix C contains a detailed mathematical analysis and numerical verification of the required conditions for the Hopf bifurcation.

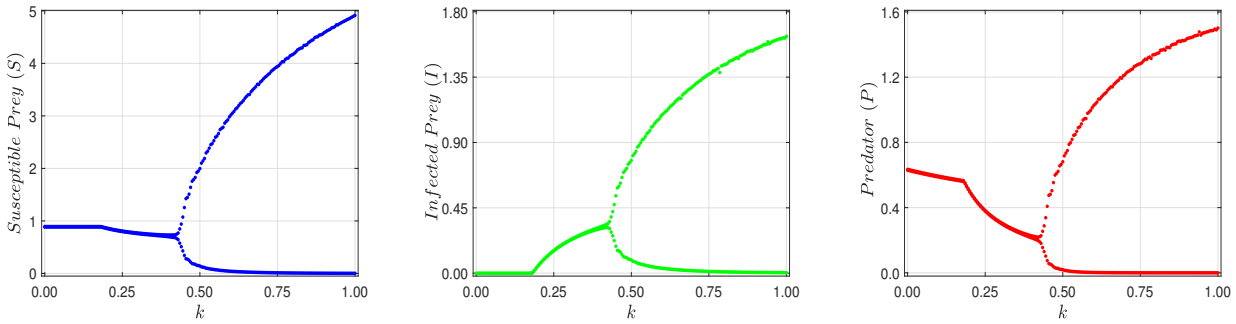

(a) Bifurcation diagram of susceptible prey (S) w.r.t. cost of fear (k).

(b) Bifurcation diagram of infected prey (I) w.r.t. cost of fear (k).

(c) Bifurcation diagram of predator (P) w.r.t. cost of fear (k).

Figure 3. System (1) experiences a supercritical Hopf bifurcation as the interior loses its stability when we increase k. All other parameters are taken from Table 1.

5. Discussion

Fear of predators lowers the prey's birth rate in a general prey-predator system where the prey population is infected. Finding the effect of dread on the coexistence of such an eco-epidemiological system is our goal. The available research [34–36] demonstrates that stable coexistence between susceptible prey, infected prey, and the predator is possible when the predator benefits more from the consumption of infected prey than the susceptible. However, since we believe that eating diseased prey is less advantageous for the predator than eating susceptible prey, it can occasionally have a detrimental effect on the predator's health (e.g., in California, a significant number of pelican birds perished after eating contaminated seafood between 1992–1996). Sasmal [22] demonstrated that the coexistence of such an eco-epidemiological system is also improved and aided by the dread of predators.

The dynamical results of system (1) will now be compared with those of other models, either by removing or incorporating certain important components. These include the elimination of the cost

of fear (subsection 5.1), incorporating the Allee effect in predator population growth (5.2), and the relaxation of certain assumptions in system (1) to a more generic version of it (5.3). The purpose of the following subsections is to validate and generalize the system (1) outcomes and answer the questions addressed in the introduction.

5.1. System (1) *without the cost of fear*

The dynamical result of system (1) is verified when there is no fear effect of predators on prey, as our primary focus is on the influence of predator fear in an eco-epidemiological model. When we eliminate the cost of fear from the prey population's growth, system (1) becomes

$$\begin{aligned} \frac{dS}{dt} &= S\left(r - d_1 - d_2(S+I) - \frac{\beta I}{S+I} - aP\right), \\ \frac{dI}{dt} &= I\left(\frac{\beta S}{S+I} - aP - \mu\right), \\ \frac{dP}{dt} &= P\Big(bS + \alpha I - d_3\Big). \end{aligned} \tag{9}$$

System (9) has four non-zero equilibria. The existence and stability conditions of those are listed in Table 2.

Table 2. Existence and stability conditions for the equilibria of the system (9).

Equilibrium	Existence conditions	Stability conditions
$E_S = \left(\frac{r-d_1}{d_2}, 0, 0\right)$	$r > d_1$	$R_0 < 1$ & $R_d < \frac{d_2}{r-d_1}$
$E_{SI} = (\mu S_2, \mu(R_0-1)S_2, 0)$	$1 < R_0 < 1 + \frac{r-d_1}{\mu}$	$\max\left\{1, R_0^{SI}\right\} < R_0 < 1 + \frac{r-d_1}{\mu}$
$E_{SP} = \left(\frac{1}{R_d}, 0, \frac{(r-d_1)R_d - d_2}{aR_d}\right)$	$R_d > \frac{d_2}{r-d_1}$	$R_d > \max\left\{\frac{d_2}{r-d_1}, \frac{d_2}{r-d_1-\mu(R_0-1)}\right\}$
$E^* = \left(S_1^*, I_1^*, P_1^*\right)$	$d_2 < R_d\left[r - d_1 - \mu(R_0-1)\right] < \frac{bd_3R_0}{b+\alpha(R_0-1)}$	Never stable

where $S_2 = \frac{r-d_1-\mu(R_0-1)}{\mu d_2 R_0}$, $S_1^* = \frac{bd_2 - \alpha R_d\left[r-d_1-\mu(R_0-1)\right]}{d_2R_d(b-\alpha)}$, $I_1^* = \frac{b\left[R_d\left\{r-d_1-\mu(R_0-1)\right\}-d_2\right]}{d_2R_d(b-\alpha)}$, $P_1^* = \frac{\mu\left[bd_2R_0 - R_d\left\{b+\alpha(R_0-1)\right\}\left\{r-d_1-\mu(R_0-1)\right\}\right]}{aR_d(b-\alpha)\left[r-d_1-\mu(R_0-1)\right]}$, and R_0^{SI} is the positive root of the quadratic equation

$$\alpha\mu R_dR_0^2 + \left[b\left(\mu R_d + d_2\right) + aR_d\left(r - d_1 - 2\mu\right)\right]R_0 + R_d\left[\alpha(\mu - r + d_1) - b(\mu + r - d_1)\right] = 0.$$

From Table 2, it is seen that when there is no fear of predators, a stable coexistence of susceptible prey, infected prey, and predator is impossible, but the incorporation of fear of predators can significantly change the stability of the coexistence equilibrium of such an eco-epidemiological system as system (1) has stable coexistence equilibrium. According to biology, in the absence of predator fear, the system either converges to a state devoid of infections or predators, as cohabitation is unstable, even with positive starting population densities of susceptible prey, diseased prey, and predator. Being free of infections is desirable, while being devoid of predators is undesirable. An eco-epidemiological system that incorporates fear of predators can help maintain population cohabitation, which is crucial to avoiding such a situation.

5.2. *System* (1) *with a weak Allee effect in the predator*

Sasmal and Chattopadhyay [34] considered the weak Allee effect in the growth of predator population and concluded that with or without the Allee effect, stable coexistence between susceptible prey, infected prey, and predator is impossible. Kang et al. [36] considered a strong Allee effect in the growth of prey population and concluded a similar result, that with or without the Allee effect, stable coexistence of such an eco-epidemiological system is impossible. Sasmal et al. [35] modified the system of Kang et al. [36] by considering that intraspecific competition induced additional deaths of predators which caused the hydra effect [39–41] that can increase the population density of the predator at the equilibrium with an increase in the mortality (in [35], the mortality is the intraspecfic death of predators) promoting the coexistence of such eco-epidemiological systems with susceptible prey, infected prey, and predator.

In this subsection, we compare our studied system (1) in the presence of a weak Allee effect in the growth of the predator population. For that, we have considered the following system:

$$\begin{aligned}\frac{dS}{dt} &= S\left[\frac{r}{1+kP} - d_1 - d_2\big(S+I\big) - \frac{\beta I}{S+I} - aP\right],\\ \frac{dI}{dt} &= I\left[\frac{\beta S}{S+I} - aP - \mu\right],\\ \frac{dP}{dt} &= P\left[\Big(bS+\alpha I\Big)\left(\frac{P}{P+\theta}\right) - d_3\right].\end{aligned} \tag{10}$$

Here θ is the weak Allee parameter. If we neglect θ (that is, if $\theta = 0$), then system (10) transforms to system (1), and the coexistence equilibrium follows the dynamics as described in Theorems 3.1 and 3.4. But whenever $\theta \neq 0$, system (10) has one stable interior equilibrium (see Figure 4) out of two interior equilibria that exist. We can consider system (10) as a modification of the system studied in [34] with the incorporation of the cost of fear in the birth rate of prey. As Sasmal et al. [35] showed that the hydra effect can promote the coexistence of such eco-epidemiological models, we show that the fear effect can also promote the coexistence of such eco-epidemiological systems.

From Figure 4, we can conclude that the stable coexistence between susceptible prey, infected prey, and predator is promoted when we incorporate the cost of fear of predators in the growth of prey, and this result will not alter if, additionally, we add Allee effects in the predator population.

Interestingly, even though susceptible prey, infected prey, and predators coexist in both the system (1) and the system studied in [35], the dynamics of the former are simpler than those of the latter since the former does not support any multistability between the system's equilibria and has unique interior equilibrium, while the latter supports bistability between infection-free equilibrium and predator-free equilibrium and provides two interior equilibria. Since the Allee effect does not influence the stability of the coexistence equilibrium, such complexity may arise due to the inclusion of the Allee effect. In biology, if a system exhibits bistability between two equilibria, it can reach any of those stable equilibria under the same parametric conditions, based on the initial population densities. In contrast, under specific parametric conditions, the system should converge to a single stable equilibrium. Therefore, in such an eco-epidemiological system, including fear of predators can greatly improve species preservation policy.

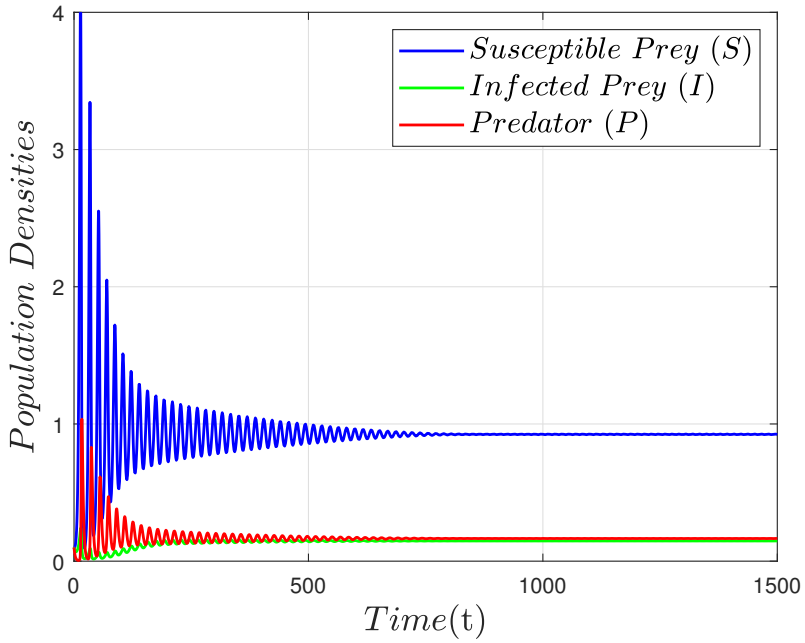

Figure 4. Time series of susceptible prey (blue), infected prey (green), and predator (red) of the system (10) with parameters $\theta = 0.001$, $R_0 = 1.5$, $R_d = 1.0$, $k = 5.0$, and all other parameters are taken from Table 1. System (10) converges to stable interior equilibrium for initial condition $(S,\ I,\ P) = (0.1,\ 0.1,\ 0.1)$.

5.3. *System* (1) *with different capture rates and different inter-specific competitions for susceptible prey and infected prey*

Here we present an expanded version of system (1), in which susceptible prey and infected prey are not constrained by factors like equal resource competition or equal predator's capture rate of susceptible and infected prey. Some literature suggests that the infected prey are easier to catch compared to susceptible prey [31, 42]. But in general, susceptible prey are more competitive in resource consumption than infected prey as the disease physically weakens them. Thus we modify system (1) as

$$\begin{aligned} \frac{dS}{dt} &= S\left[\frac{r}{1+kP} - d_1 - d_2\big(S+\delta I\big) - \frac{\beta I}{S+I} - a_1 P\right], \\ \frac{dI}{dt} &= I\left[\frac{\beta S}{S+I} - a_2 P - \mu\right], \\ \frac{dP}{dt} &= P\Big[bS + \alpha I - d_3\Big]. \end{aligned} \tag{11}$$

Here $a_1,\ a_2$ $(a_1 \le a_2)$ denotes the capture rates for susceptible prey and infected prey by the predators, respectively, and δ (≤ 1) is the coefficient that takes into account the reduced competition for resources between the infected and susceptible prey populations. If $\delta = 1$ and $a_1 = a_2 = a$, system (11) will reduce to our studied system (1).

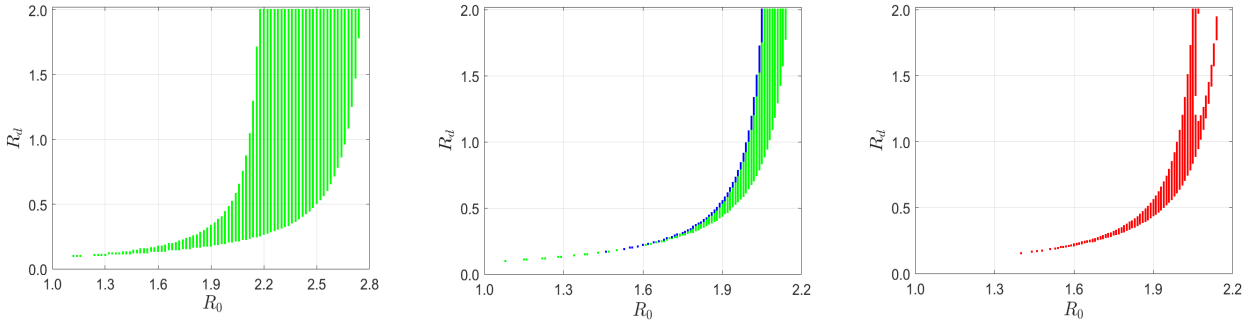

(a) Region of existence of interior for system (11) when $k = 0$.

(b) Region of existence of interior(s) for system (11) when $k = 1$.

(c) Region of stability of interior for system (11) when $k = 1$.

Figure 5. The existence and stability of the interior of system (11) for $a_1(= 0.6) \leq a_2(= 0.9)$, $b(= 0.45) \geq \alpha(= 0.25)$, $\delta \leq 1$, and all other parameters are taken from Table 1. When there is no fear (i.e., $k = 0$), there exists a unique unstable interior (Figure 5(a)) but when there is fear of predators ($k = 1$), there exist one (green) or two (blue) interiors (Figure 5(b)), one of which is stable (red region in Figure 5(c)).

Case I: Suppose that the net gain of predators for devouring susceptible prey (b) is greater than the net gain for consuming the population of diseased prey (α), that is, $b \geq \alpha$ (i.e., $-\infty < \alpha \leq b$), even if the capture rate of infected prey is larger than that of susceptible prey ($a_1 \leq a_2$). Also, we consider $\delta \leq 1$, that is, the infected prey competes less or equally with the susceptible prey for resources. Then we obtain the following outcomes regarding the stability of equilibria.

1) There exists a unique interior, which is always unstable without the influence of predator fear ($k = 0$). The green region in Figure 5(a) represents the region of existence of unique unstable equilibrium.

2) In the presence of predator fear ($k = 1$), there exist two interiors. The blue and green regions in Figure 5(b) represent the region of existence of two and one interior(s), respectively. Also, now there is a stable interior (the red region in Figure 5(c)) equilibrium.

From Figure 5, we can conclude that the cost of fear can promote the coexistence of susceptible prey, infected prey, along with the predator in a complex eco-epidemiological system either by creating new interior(s) or changing the stability from unstable to stable.

Case II: We now examine the scenario in which the net benefit of eating infected prey is greater than that of eating susceptible prey because infected prey is easier to catch—that is, $a_1 < a_2$ and c' is always positive, with $c' \leq c$ (i.e., the conversion efficiency is still lower for infected prey than susceptible prey); however, $c'a_2 > ca_1$, i.e., $\alpha > b$. Then there are two interiors, one of which is always steady, whether or not the cost is the dread of predators. However, as the intensity of anxiety grows, so does the zone of stability (see Figure 6).

The expansion of the region of stability, which indicates the stability of the interior for greater ranges of the parameters involved, or the transformation of the unstable equilibrium into a stable one, implies that the cost of predation fear can facilitate the cohabitation of the three populations. Here,

the three populations' coexistence is possible without fear if predator gain from the higher competitive prey is lower than the other [31, 34, 36]. However, fear can increase the region of stability. In contrast to system (1), this subsection illustrates the predator fear in a broader eco-epidemiological system. It has been demonstrated that, regardless of the predator's gain from susceptible and diseased prey and their capturing rate, predator fear may always improve the stability and existence of the coexisting equilibrium of such systems.

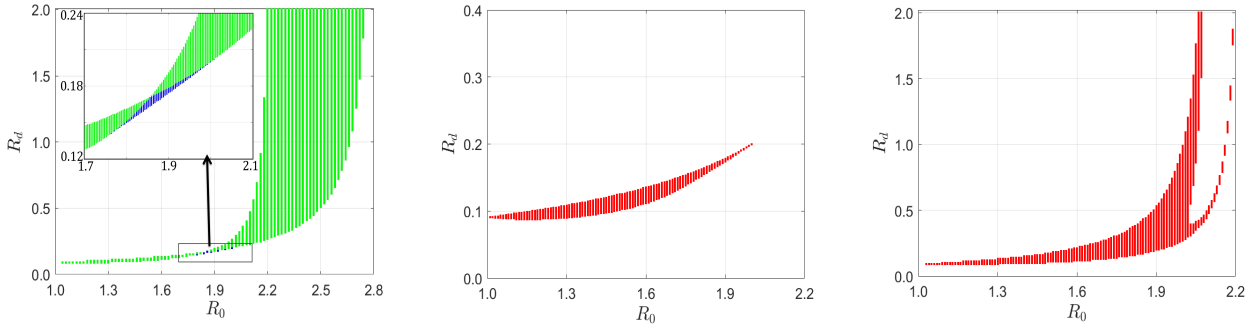

(a) Region of existence of interior(s) for system (11) when $k = 0$.

(b) Region of stability of interior(s) for system (11) when $k = 0$.

(c) Region of stability of interior for system (11) when $k = 1$.

Figure 6. The existence and stability of the interior(s) of system (11) for $a_1(= 0.6) < a_2(= 0.9)$, $b(= 0.25) < \alpha(= 0.45)$, $\delta(= 0.5) \leq 1$, and all other parameters are taken from Table 1. Without the cost of fear (i.e., $k = 0$), there exists one (green) or two (blue) interiors depicted in Figure 6(a), and the stability region for $k = 0$ is given in Figure 6(b). But when $k = 1$, the stability region is increased and given in Figure 6(c).

Although this study focuses on the role of predator-induced fear under simplified assumptions, such as Holling type I functional response, and later compared with weak Allee effects, we acknowledge that more realistic ecological complexities may significantly improve the system complexity. Adopting Holling type II or III functional responses could introduce saturation or nonlinear prey handling dynamics, which can potentially give richer dynamics. However, the stabilizing role of fear on the eco-epidemiological system will not change with Holling type II/III functional response. Richer dynamical studies with more complex functional responses can be a potential future direction. Moreover, the interaction of fear with other ecological parameters, including disease transmission rates, predator mortality, and resource competition, may require deeper investigation and provide different outcomes. Additionally, analyzing strong Allee effects and their interaction with fear could uncover important thresholds for persistence and extinction of species. These aspects represent promising directions for future research to enrich the ecological relevance and generality of such eco-epidemiological models.

6. Conclusions

We analyze a general eco-epidemiological system with infection in the prey population. We assume that our proposed system (1) follows the frequency-dependent disease transmission law and that the infected prey population has no contribution to the new births, but the infected prey equally competes

for resources with susceptible prey. Also, we consider that the net gain of predators for consuming infected prey is lesser than consuming susceptible prey. We incorporate the cost of fear of predators into the birth of the prey. Accessing the system's behavior at the origin is not easy in such a system, since the systems connected to the ratio-dependent transmission rate are not defined there. We have used time-scale desingularization and polar blow-up techniques to remove the singularity of the origin and analyze the dynamical behavior of the extinction equilibrium of system (1). Additionally, we analyze the stability of each equilibrium of system (1), where the cost of fear (k), the basic reproduction number (R_0), and the disease-free demographic reproduction number of predators (R_d) play crucial roles. System (1) has unique coexistence equilibrium which can be locally asymptotically stable or it can have oscillatory coexistence. By analyzing and numerically verifying system (1), and by discussing and comparing the results obtained with the outcomes from models (9)–(11), we answer the questions raised in the introduction.

From Table 2, we can say that without the cost of fear, system (9) has no stable coexistence between susceptible prey, infected prey, and predator. In contrast, after adding the cost of fear into the birth of prey population, system (1) exhibits oscillatory coexistence and stable coexistence between the species. From this, we can conclude that the cost of fear of predators can promote the coexistence of such an eco-epidemiological system, which answers the first question.

We study system (10), which exhibits stable coexistence, whereas Sasmal and Chattopadhyay [34] showed that without the cost of fear, system (10) could not have stable coexistence in such an eco-epidemiological system. Thus, we conclude that with or without the Allee effect, the cost of fear of predators can promote coexistence in such an eco-epidemiological system, which answers the second question.

Our conclusion is the same, i.e., fear can promote the three species' coexistence even if we remove the two vital assumptions, equal competitive abilities of susceptible and infected prey, and equal capture rates of both prey by predator. By studying the more general model (11), we answer the third question.

This research offers important ecological insights into how long-term species dynamics may be impacted by behavioral reactions to predation, particularly the decrease in prey birth rates carried on by fear. The model shows how fear, a non-lethal but significant ecological element, may make otherwise unstable systems stable and encourage the existence of all interacting populations. The results of coexistence are noteworthy because they show how resilient fear-driven processes are, even when traditional presumptions like predator feeding preferences or prey competitiveness are loosened. These results highlight how behavioral ecology should be incorporated into eco-epidemiological models to better understand the stability of real-world ecosystems.

Use of AI tools declaration

The authors declare they have not used Artificial Intelligence (AI) tools in the creation of this article.

Acknowledgments

RD acknowledges the financial support from the Ministry of Education (MoE), Government of India. The authors gratefully acknowledge the valuable comments and suggestions provided by the

anonymous reviewers and editor, which strengthen the biological interpretation of the findings, model assumptions, and theoretical analysis.

Conflict of interest

The authors declare that they have no conflict of interest.

References

1. A. Lotka, Elements of Physical Biology, *Nature*, **116** (1925), 461. https://doi.org/10.1038/116461b0
2. V. Volterra, Fluctuations in the abundance of a species considered mathematically, *Nature*, **118** (1926), 558–560. https://doi.org/10.1038/118558a0
3. S. L. Lima, L. M. Dill, Behavioral decisions made under the risk of predation: A review and prospectus, *Can. J. Zool.*, **68** (1990), 619–640. https://doi.org/10.1139/z90-092
4. J. P. Suraci, M. Clinchy, L. M. Dill, D. Roberts, L. Y. Zanette, Fear of large carnivores causes a trophic cascade, *Nat. Commun.*, **7** (2016), 10698. https://doi.org/10.1038/ncomms10698
5. S. K. Sasmal, Y. Takeuchi, Dynamics of a predator-prey system with fear and group defense, *J. Math. Anal. Appl.*, **481** (2020), 123471. https://doi.org/10.1016/j.jmaa.2019.123471
6. A. Sih, H. J. Chung, I. Neylan, C. Ortiz-Jimenez, O. Sakai, R. Szeligowski, Fear generalization and behavioral responses to multiple dangers, *Trends Ecol. Evol.*, **38** (2023), 369–380. https://doi.org/10.1016/j.tree.2022.11.001
7. K. Hadeler, H. Freedman, Predator-prey populations with parasitic infection, *J. Math. Biol.*, **27** (1989), 609–631. https://doi.org/10.1007/BF00276947
8. J. Chattopadhyay, O. Arino, A predator-prey model with disease in the prey, *Nonlinear Anal.*, **36** (1999), 747–766. https://doi.org/10.1016/S0362-546X(98)00126-6
9. J. Chattopadhyay, S. Pal, Viral infection on phytoplankton-zooplankton system—A mathematical model, *Ecol. Modell.*, **151** (2002), 15–28. https://doi.org/10.1016/S0304-3800(01)00415-X
10. N. Bairagi, P. K. Roy, J. Chattopadhyay, Role of infection on the stability of a predator-prey system with several response functions—A comparative study, *J. Theor. Biol.*, **248** (2007), 10–25. https://doi.org/10.1016/j.jtbi.2007.05.005
11. H. W. Hethcote, The mathematics of infectious diseases, *SIAM Rev.*, **42** (2000), 599–653. https://doi.org/10.1137/S0036144500371907
12. A. P. Dobson, P. J. Hudson, Parasites, disease and the structure of ecological communities, *Trends Ecol. Evol.*, **1** (1986), 11–15. https://doi.org/10.1016/0169-5347(86)90060-1
13. S. M. Moore, E. T. Borer, P. R. Hosseini, Predators indirectly control vector-borne disease: Linking predator-prey and host-pathogen models, *J. R. Soc. Interface*, **7** (2010), 161–176. https://doi.org/10.1098/rsif.2009.0131
14. S. Creel, D. Christianson, Relationships between direct predation and risk effects, *Trends Ecol. Evol.*, **23** (2008), 194–201. https://doi.org/10.1016/j.tree.2007.12.004

15. W. Cresswell, Predation in bird populations, *J. Ornithol.*, **152** (2011), 251–263. https://doi.org/10.1007/s10336-010-0638-1

16. L. Y. Zanette, A. F. White, M. C. Allen, M. Clinchy, Perceived predation risk reduces the number of offspring songbirds produce per year, *Science*, **334** (2011), 1398–1401. https://doi.org/10.1126/science.1210908

17. C. S. Holling, The functional response of predators to prey density and its role in mimicry and population regulation, *Mem. Entomol. Soc. Can.*, **97** (1965), 5–60. https://doi.org/10.4039/entm9745fv

18. C. S. Holling, Some characteristics of simple types of predation and parasitism1, *Can. Entomol.*, **91** (1959), 385–398. https://doi.org/10.4039/Ent91385-7

19. M. E. Gilpin, Do hares eat lynx?, *Am. Nat.*, **107** (1973), 727–730. https://doi.org/10.1086/282870

20. V. Krivan, Effects of optimal antipredator behavior of prey on predator-prey dynamics: The role of refuges, *Theor. Popul. Biol.*, **53** (1998), 131–142. https://doi.org/10.1006/tpbi.1998.1351

21. X. Wang, L. Zanette, X. Zou, Modelling the fear effect in predator-prey interactions, *J. Math. Biol.*, **73** (2016), 1179–1204. https://doi.org/10.1007/s00285-016-0989-1

22. S. K. Sasmal, Population dynamics with multiple Allee effects induced by fear factors—A mathematical study on prey-predator interactions, *Appl. Math. Modell.*, **64** (2018), 1–14. https://doi.org/10.1016/j.apm.2018.07.021

23. M. Hossain, N. Pal, S. Samanta, Impact of fear on an eco-epidemiological model, *Chaos Solitons Fractals*, **134** (2020), 109718. https://doi.org/10.1016/j.chaos.2020.109718

24. K. Sarkar, S. Khajanchi, An eco-epidemiological model with the impact of fear, *Chaos Int. J. Nonlinear Sci.*, **32** (2022), 83126. https://doi.org/10.1063/5.0099584

25. M. Begon, M. Bennett, R. G. Bowers, N. P. French, S. Hazel, J. Turner, A clarification of transmission terms in host-microparasite models: Numbers, densities and areas, *Epidemiol. Infect.*, **129** (2002), 147–153. https://doi.org/10.1017/s0950268802007148

26. M. Krupa, P. Szmolyan, Extending geometric singular perturbation theory to nonhyperbolic points—fold and canard points in two dimensions, *SIAM J. Math. Anal.*, **33** (2001), 286–314. https://doi.org/10.1137/S0036141099360919

27. F. Dumortier, J. Llibre, C. J. Artés, *Qualitative Theory of Planar Differential Systems*, Springer, 2006. https://doi.org/10.1007/978-3-540-32902-2

28. D. Xiao, S. Ruan, Global dynamics of a ratio-dependent predator-prey system, *J. Math. Biol.*, **43** (2001), 268–290. https://doi.org/10.1007/s002850100097

29. D. Bai, J. Wu, B. Zheng, J. Yu, Hydra effect and global dynamics of predation with strong Allee effect in prey and intraspecific competition in predator, *J. Differ. Equations*, **384** (2024), 120–164. https://doi.org/10.1016/j.jde.2023.11.017

30. Y. Ichida, Y. Nakata, Global dynamics of a simple model for wild and sterile mosquitoes, *Math. Biosci. Eng.*, **21** (2024), 7016–7039. https://doi.org/10.3934/mbe.2024308

31. H. W. Hethcote, W. Wang, L. Han, Z. Ma, A predator-prey model with infected prey, *Theor. Popul. Biol.*, **66** (2004), 259–268. https://doi.org/10.1016/j.tpb.2004.06.010

32. A. Deredec, F. Courchamp, Combined impacts of Allee effect and parasitism, *Oikos*, **112** (2006), 667–679. https://doi.org/10.1111/j.0030-1299.2006.14243.x

33. F. M. Hilker, M. Langlais, H. Malchow, The Allee effect and infectious diseases: Extinction, multistability, and the (dis-)appearance of oscillations, *Am. Nat.*, **173** (2009), 72–88. https://doi.org/10.1086/593357

34. S. K. Sasmal, J. Chattopadhyay, An eco-epidemiological system with infected prey and predator subject to the weak Allee effect, *Math. Biosci.*, **246** (2013), 260–271. https://doi.org/10.1016/j.mbs.2013.10.005

35. S. K. Sasmal, Y. Kang, J. Chattopadhyay, Intra-specific competition in predator can promote the coexistence of an eco-epidemiological model with strong Allee effects in prey, *BioSystems*, **137** (2015), 34–44. https://doi.org/10.1016/j.biosystems.2015.09.003

36. Y. Kang, S. K. Sasmal, A. R. Bhowmick, J. Chattopadhyay, Dynamics of a predator-prey system with prey subject to Allee effects and disease, *Math. Biosci. Eng.*, **11** (2014), 877–918. https://doi.org/10.3934/mbe.2014.11.877

37. J. Chattopadhyay, P. Srinivasu, N. Bairagi, Pelicans at risk in Salton Sea—An eco-epidemiological model-II, *Ecol. Modell.*, **167** (2003), 199–211. https://doi.org/10.1016/S0304-3800(03)00187-X

38. S. Jha, *Grey Pelicans Die in Droves in Srikakulam*, Down Earth, 2022.

39. P. A. Abrams, H. Matsuda, The effect of adaptive change in the prey on the dynamics of an exploited predator population, *Can. J. Fisher. Aquat. Sci.*, **62** (2005), 758–766. https://doi.org/10.1139/f05-051

40. P. A. Abrams, When does greater mortality increase population size? The long history and diverse mechanisms underlying the hydra effect, *Ecol. Lett.*, **12** (2009), 462–474. https://doi.org/10.1111/j.1461-0248.2009.01282.x

41. M. Sieber, F. M. Hilker, The hydra effect in predator-prey models, *J. Math. Biol.*, **64** (2012), 341–360. https://doi.org/10.1007/s00285-011-0416-6

42. J. Moore, *Parasites and the Behavior of Animals*, Oxford University Press, New York, 2002. https://doi.org/10.1093/oso/9780195084412.001.0001

Appendix

Appendix A

The signs of the coefficients of Eq (5) are as follows:

$$A = d_2\,(b-\alpha)\left[b(a-\mu k) - a\alpha - \alpha k\mu(R_0-1)\right] \implies A < 0 \iff R_0 - 1 > \frac{a(b-\alpha) - b\mu k}{\alpha\mu k}.$$

B is the following quadratic function of $R_0 - 1$:

$$\begin{aligned}\phi_B(R_0-1) \;=\; & -\mu^2\alpha k R_d\,(R_0-1)^2 - \mu\left[\{k\,(b\mu+\alpha d_1) - a(b-\alpha)\}\,R_d - k d_2\,(b-2\alpha)\right](R_0-1)\\ & -\{a(b-\alpha)(r-d_1) + b d_1\mu k\}\,R_d + d_2\left[2a(b-\alpha) - b\mu k\right],\end{aligned}$$

$$= -\mu^2\alpha k R_d(R_0-1)^2 + B_1(R_0-1) + B_2 \text{ (say)},$$

Then $B_1^2 + 4\alpha\mu^2 k R_d B_2 \le 0 \implies B < 0$.

If $B_1^2 + 4\alpha\mu^2 k R_d B_2 > 0$, then there are the following scenarios:

- $B_2 > 0$: The equation $\phi_B(R_0-1) = 0$ has one positive root $R_0^{(2)}$ (say), consequently, $B > 0$ if $1 < R_0 < 1 + R_0^{(2)}$, and $B < 0$ if $R_0 > 1 + R_0^{(2)}$.
- $B_2 \le 0$ and $B_1 \le 0 : \implies B < 0$ for $R_0 > 1$.
- $B_2 < 0$ and $B_1 > 0$: The equation $\phi_B(R_0-1) = 0$ has two positive roots $R_0^{(1)}, R_0^{(2)}$ (say), and consequently, $B > 0$ if $1 + R_0^{(1)} < R_0 < 1 + R_0^{(2)}$, and $B < 0$ if $1 < R_0 < 1 + R_0^{(1)}$, or $R_0 > 1 + R_0^{(2)}$.
- $B_2 = 0$ and $B_1 > 0$: The root $R_0^{(1)}$ merges to zero, and consequently, $B > 0$ if $1 < R_0 < 1 + R_0^{(2)}$, and $B < 0$ if $R_0 > 1 + R_0^{(2)}$.

Here, $B_1 < 0 \iff R_d > \dfrac{kd_2(b-2\alpha)}{k(b\mu+\alpha d_1) - a(b-\alpha)}$, and $B_2 < 0 \iff R_d > \dfrac{d_2\left[2a(b-\alpha) - b\mu k\right]}{b\mu k d_1 + a(b-\alpha)(r-d_1)}$.

And $R_0^{(1),(2)} = \dfrac{-B_1 \pm \sqrt{B_1^2 + 4\alpha\mu^2 k R_d B_2}}{-2\alpha\mu^2 k R_d}$, $[R_0^{(1)} < R_0^{(2)}]$ provided $B_1^2 + 4\alpha\mu^2 k R_d B_2 > 0$.

$$\begin{aligned}
\text{Now,}\quad B_1^2 + 4\alpha\mu^2 k R_d B_2 &= \mu^2\left[\{k(\alpha d_1 - b\mu) + a(b-\alpha)\}^2 - 4ak\alpha r(b-\alpha)\right]R_d^2 \\
&\quad -2\mu^2 d_2 k\left[\alpha(2\alpha-b)(a-d_1k) + b^2(\mu k - a)\right]R_d + \mu^2k^2d_2^2(2\alpha-b)^2, \\
\text{alternatively,}\quad &= \mu^2\left[\{\alpha(a-d_1k)R_d - kd_2(2\alpha-b)\}^2 + \{b(\mu k-a)R_d - \mu k b d_2\}^2\right] \\
&\quad +\mu^2\left[2\left\{bk\mu(ab-\alpha d_1) + a\alpha k\Big(\alpha d_1 - 2r(b-\alpha)\Big) - b\alpha\right\}R_d^2 - k^2b^2d_2^2\right].
\end{aligned}$$

Now, C is the following quadratic function of $R_0 - 1$:

$$\phi_C(R_0-1) = \mu^2 k R_d\,(R_0-1)^2 + \mu\left\{kd_2 + R_d\,(a + d_1k)\right\}(R_0-1) - a\left\{(r-d_1)\,R_d - d_2\right\}.$$

If $R_d \le \dfrac{d_2}{r-d_1}$ then $C > 0$.

Again, if $R_d > \dfrac{d_2}{r-d_1}$, then the equation $\phi_C(R_0-1) = 0$ has one positive root $R_0^{(3)}$ (say), and consequently, $C < 0$ if $1 < R_0 < 1 + R_0^{(3)}$, and $C > 0$ if $R_0 > 1 + R_0^{(3)}$, whereas,

$$R_0^{(3)} = \frac{-\left[(a+d_1k)R_d + d_2k\right] + \sqrt{\left[(a-d_1k)R_d - d_2k\right]^2 + 4akrR_d^2}}{2\mu k R_d}.$$

Appendix B

Jacobian matrix (8) elements of system (1):

$$\begin{aligned}
F_S^{(1)} &= -d_2 + \frac{\mu R_0 I}{(S+I)^2}, & F_I^{(1)} &= -\left(d_2 + \frac{\mu R_0 S}{(S+I)^2}\right), & F_P^{(1)} &= -\left(a + \frac{rk}{(1+kP)^2}\right), \\
F_S^{(2)} &= \frac{\mu R_0 I}{(S+I)^2}, & F_I^{(2)} &= -\frac{\mu R_0 S}{(S+I)^2}, & F_P^{(2)} &= -a, \\
F_S^{(3)} &= b, & F_I^{(3)} &= \alpha, & F_P^{(3)} &= 0.
\end{aligned}$$

Appendix C

The Jacobian at the interior has the following characteristic equation

$$\lambda^3 + A_1\lambda^2 + A_2\lambda + A_3 = 0.$$

Then the Hopf bifurcation can occur when $A_1A_2 = A_3$, provided the transversality condition $\frac{d}{dk}(A_1A_2 - A_3) \neq 0$ is satisfied. For a detailed mathematical calculation, we proceed as follows:

Since the interior equilibrium depends on the positive solution of the quadratic equation $Ax^2 + Bx + C = 0$, where all the coefficients $A,\ B,\ C$ (expressions are given in Theorem 3.1) are functions of the bifurcating parameter k, we use implicit differentiation to find

$$\frac{dX^*}{dk} = -\frac{\frac{dA}{dk}X^{*2} + \frac{dB}{dk}X^* + \frac{dC}{dk}}{2AX^* + B}$$

We can use the above expression to find the derivatives of expressions of $S^*,\ I^*$, and P^* (expressions are given in Theorem 3.1) as

$$\begin{aligned}
\frac{dS^*}{dk} &= -\frac{\alpha}{R_d}\frac{dX^*}{dk},\\
\frac{dI^*}{dk} &= \frac{b}{R_d}\frac{dX^*}{dk}, \text{and}\\
\frac{dP^*}{dk} &= -\frac{b\mu R_0}{a\{1 + (b-\alpha)X^*\}^2}\frac{dX^*}{dk}.
\end{aligned}$$

The coefficients of the characteristic equation of the Jacobian at the interior are given in proof of Theorem 3.4. We can calculate the following derivatives using the above equations and the expressions of $S^*,\ I^*$, and P^* given in Theorem 3.1:

$$\begin{aligned}
\frac{dA_1}{dk} &= d_1\frac{dS^*}{dk},\\
\frac{dA_2}{dk} &= \frac{ab}{R_d}\frac{dP^*}{dk} + \frac{br}{(1+kP^*)^3}\left[(1+kP^*)kP^*\frac{dS^*}{dk} + S(1-kP^*)\left(P^* + k\frac{dP^*}{dk}\right)\right]\\
&\quad + \frac{\mu d_2 R_0}{(S^*+I^*)^2}\left[S^{*2}\frac{dI^*}{dk} + I^{*2}\frac{dS^*}{dk}\right],\\
\frac{dA_3}{dk} &= \left[\frac{br\mu kR_o}{R_d\{(S^*+I^*)(1+kP^*)\}^2} - ad_2(b-\alpha)\right]\left(S^*I^*\frac{dP^*}{dk} + S^*\frac{dI^*}{dk}P^* + \frac{dS^*}{dk}I^*P^*\right)\\
&\quad - \frac{br\mu kR_0S^*I^*P^*}{R_d\{(S^*+I^*)(1+kP^*)\}^3}\left[(S^*+I^*)\left(P^* + 2k\frac{dP^*}{dk}\right) - 2(1+kP^*)\left(\frac{dS^*}{dk} + \frac{dI^*}{dk}\right)\right].
\end{aligned}$$

The transversality condition for Hopf bifurcation in a three-dimensional system can be written as

$$\frac{d}{dk}(A_1A_2 - A_3) \neq 0$$

$$\implies A_1 \frac{dA_2}{dk} + \frac{dA_1}{dk} A_2 - \frac{dA_3}{dk} \neq 0.$$

Now, finally, we can find the value of k at which the Hopf bifurcation will occur by plotting the expression $A_1A_2 - A_3$ with respect to k. When the graph crosses the $k-$axis, provide the bifurcation point. We can also plot the transversality condition with respect to k, and verify that at the bifurcating point, it is nonzero or not. Figure A1 gives the Hopf bifurcation point value of $k \approx 0.435$, which satisfies the Hopf bifurcation point of Figure 3 in the manuscript.

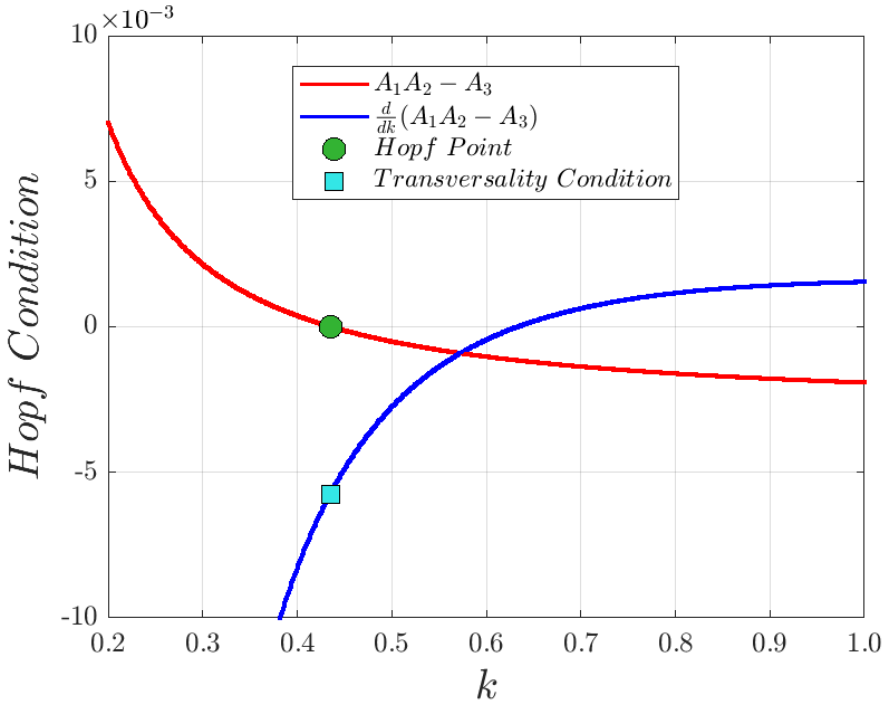

Figure A1. Figure shows the Hopf bifurcation condition and the transversality condition for it in red and blue colour, respectively.